NOAA Technical Memorandum NESS 21

U.S. DEPARTMENT OF COMMERCE
National Oceanic and Atmospheric Administration
National Environmental Satellite Service

Geostationary Satellite Position and Attitude Determination Using Picture Landmarks

WILLIAM J. DAMBECK

WASHINGTON, D.C.

August 1972

NOAA TECHNICAL MEMORANDA

National Environmental Satellite Service Series

The National Environmental Satellite Service (NESS) is responsible for the establishment and operation of the National Operational Meteorological Satellite System and of the environmental satellite systems of NOAA. The three principal Offices of NESS are Operations, Systems Engineering, and Research.

NOAA Technical Memoranda NESS series facilitate rapid distribution of material that may be preliminary in nature and which may be published formally elsewhere at a later date. Publications 1 to 25 are in the former series, ESSA Technical Memoranda, National Environmental Satellite Center Technical Memoranda (NESCTM). Beginning with 26, publications are now part of the series, NOAA Technical Memoranda, National Environmental Satellite Service (NESS).

Publications listed below are available from the National Technical Information Service, U.S. Department of Commerce, Sills Bldg., 5285 Port Royal Road, Springfield, Va. 22151. Price: $3.00 paper copy; $0.95 microfiche. Order by accession number shown in parentheses at end of each entry.

ESSA Technical Memoranda

NESCTM 6 Computer Processing of TOS Attitude Data. J. F. Gross, November 1968. (PB-182 125)

NESCTM 7 The Improved TIROS Operational Satellite. Edward G. Albert, August 1968. (PB-180 766)
Supplement No. 1. Characteristics of Direct Scanning Radiometer Data. Edward G. Albert, April 1969. (PB-183 965)

NESCTM 8 Operational Utilization of Upper Tropospheric Wind Estimates Based on Meteorological Satellite Photographs. Gilbert Jager, Walton A. Follansbee, and Vincent J. Oliver, October 1968. (PB-180 293)

NESCTM 9 Meso-Scale Archive and Products of Digitized Video Data From ESSA Satellites. Arthur L. Booth and V. Ray Taylor, October 1968. (PB-180 294)

NESCTM 10 Annotated Bibliography of Reports, Studies, and Investigations Relating to Satellite Hydrology. D. R. Baker, A. F. Flanders, and M. Fleming, June 1970. (PB-194 072)

NESCTM 11 Publications by Staff Members, National Environmental Satellite Center and Final Reports on Contracts and Grants Sponsored by the National Environmental Satellite Center 1968. January 1969. (PB-182 853)

NESCTM 12 Experimental Large-Scale Snow and Ice Mapping With Composite Minimum Brightness Charts. E. Paul McClain and Donald R. Baker, September 1969. (PB-186 362)

NESCTM 13 Deriving Upper Tropospheric Winds by Computer From Single Image, Digital Satellite Data. Charles S. Novak, June 1969. (PB-185 086)

NESCTM 14 Study of the Use of Aerial and Satellite Photogrammetry for Surveys in Hydrology. Everett H. Ramey, March 1970. (PB-191 735)

NESCTM 15 Some Aspects of the Vorticity Structure Associated With Extratropical Cloud Systems. Harold J. Brodrick, Jr., May 1969. (PB-184 178)

NESCTM 16 The Improvement of Clear Column Radiance Determination With a Supplementary 3.8μ Window Channel. William L. Smith, July 1969. (PB-185 065)

NESCTM 17 Vidicon Data Limitations. Arthur Schwalb and James Gross, June 1969. (PB-185 966)

NESCTM 18 On the Statistical Relation Between Geopotential Height and Temperature-Pressure Profiles. W. L. Smith and S. Fritz, November 1969. (PB-189 276)

NESCTM 19 Applications of Environmental Satellite Data to Oceanography and Hydrology. E. Paul McClain, January 1970. (PB-190 652)

U.S. DEPARTMENT OF COMMERCE
National Oceanic and Atmospheric Administration
National Environmental Satellite Service

NOAA Technical Memorandum NESS 21

GEOSTATIONARY SATELLITE POSITION AND ATTITUDE DETERMINATION USING PICTURE LANDMARKS

William J. Dambeck

WASHINGTON, D.C.
August 1972

National Oceanic and Atmospheric Administration
TIROS Satellites and Satellite Meteorology

ERRATA NOTICE

One or more conditions of the original document may affect the quality of the image, such as:

Discolored pages
Faded or light ink
Binding intrudes into the text

This has been a co-operative project between the NOAA Central Library and the Climate Database Modernization Program, National Climate Data Center (NCDC). To view the original document contact the NOAA Central Library in Silver Spring, MD at (301) 713-2607 x124 or Library.Reference@noaa.gov.

HOV Services
Imaging Contractor
12200 Kiln Court
Beltsville, MD 20704-1387
January 26, 2009

UDC 551.507.362.2:528.7

528	Geodesy and photogrammetry
.7	Photogrammetry
551.5	Meteorology
.507.362.2	Satellites

CONTENTS

GEOSTATIONARY SATELLITE POSITION AND ATTITUDE DETERMINATION USING PICTURE LANDMARKS

William J. Dambeck

ABSTRACT. Given a truly geostationary satellite, it is theoretically possible to determine both its position and attitude from the relative orientation of landmarks in pictures from the satellite. This paper details several attempts to exploit this possibility.

INTRODUCTION

This study, prompted by the initial planning for the Synchronous Meteorological Satellite - Geostationary Operational Environmental Satellite (SMS-GOES) series of geostationary satellites, had considerations of economy as a primary stimulus. It was generally recognized that NOAA would have the responsibility for doing its own ranging, rather than letting trilateration ranging equipment contracts. There was, of course, a monetary consideration involved: The equipment would have to be housed, personnel trained to operate and maintain it, provisions made for remote stations outside the United States, and software developed for analyzing the data. Concomitantly, it was felt that extant techniques for attitude determination, employed for Applications Technology Satellite (ATS-1 and ATS-3) operations, left much to be desired. This method relied on a combination of measured sun-pulse transit times between two slits on the satellite and polarization angle (POLANG) measurements. The procedure proved to be somewhat troublesome and admitted to an error as great as 0.5 to 1.0 degree in the spin-axis vector.

This error factor led to the development of a software program, which, while it accepts the Goddard Space Flight Center's (GSFC) satellite position measurements, made independent estimates of the attitude. Westinghouse Corporation, in particular, devoted extensive effort to a method based on earth-horizon profile measurements; NASA now employs this method. NESS evolved separate in-house approaches: One a horizon method, the other a geometrical method using picture landmark sample and line numbers as inputs. Although the horizon method was used initially as a diagnostic aid, operational use has been confined to the geometrical method which is somewhat more straightforward.

Finally, the transmission to NESS of orbital elements for ATS-1 and ATS-3, as determined by NASA, was normally delayed sufficiently to cast considerable doubt on the accuracy of the predicted positions based on these data. This was not acceptable to the NESS picture-pair wind velocity vector consortium, so it was thought desirable to have some other means for checking the accuracy of the calculated satellite positions.

For the above reasons and because it was anticipated that a landmark approach would in any event be used for finding the satellite attitude (the first SMS-GOES satellite is to include much of both landmark-rich Americas in its coverage), it was decided to investigate the feasibility of determining satellite attitude and position simultaneously. This investigation would assume as inputs the plate coordinates (sample and line numbers) of identified landmarks in the pictures to arrive at satellite position and orientation by variational procedures. Hopefully the traditional ranging approach could be abandoned.

THE SNAPSHOT APPROACH: THEORY

Initial attempts to obtain workable solutions relied on the central projection methods used in aerial photography. The sample and line number of a landmark are conceptually equivalent to the measured coordinates on a photographic plate. Consider figure 1. A satellite at S with axes x, y, z fixed in it, photographs a landmark P. The image of P falls on the plate (represented here as a diapositive) at I and has plate coordinates x_I, y_I, d. The plate is taken as perpendicular to the satellite's z-axis; the projection center is at S, the projection distance being z_I = d.

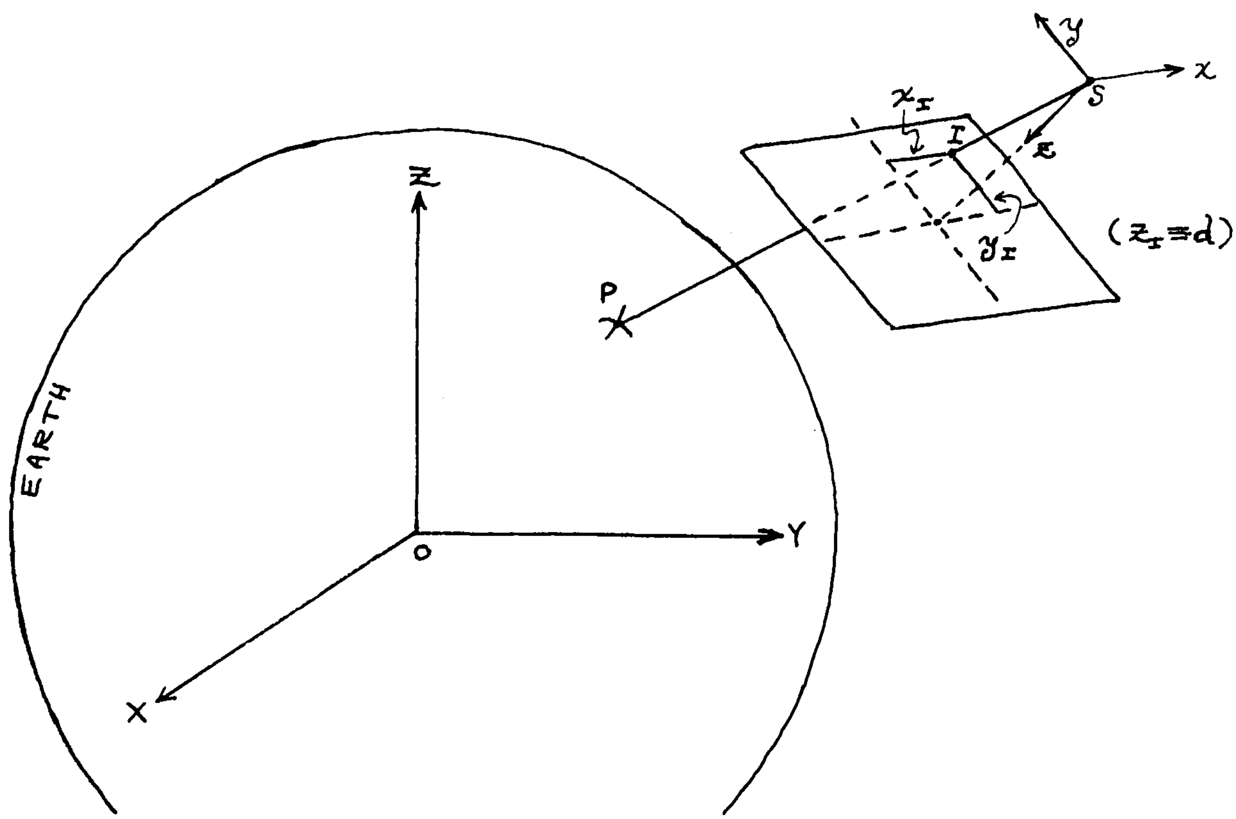

Figure 1.--Central projection.

Then the direction cosines of P as seen from S, in the x, y, z system, are:

$$l_I = \frac{x_I}{\sqrt{x_I^2 + y_I^2 + d^2}}\ , \quad m_I = \frac{y_I}{\sqrt{x_I^2 + y_I^2 + d^2}}\ , \quad n_I = \frac{d}{\sqrt{x_i^2 + y_I^2 + d^2}}\ ,$$

from which we obtain

$$\frac{l_I}{n_I} = \frac{x_I}{d}\ , \quad \frac{m_I}{n_I} = \frac{y_I}{d}, \quad \text{or}$$

$$x_I - d\left(\frac{l_I}{n_I}\right) = 0 \quad \text{and} \quad y_I - d\left(\frac{m_I}{n_I}\right) = 0\ . \tag{1}$$

The direction cosines of P as seen from S, in the earth-fixed or inertial coordinate system X, Y, Z, are:

$$l = \frac{X_p - X_s}{\sqrt{(X_p - X_s)^2 + (Y_p - Y_s)^2 + (Z_p - Z_s)^2}}\ ,$$

$$m = \frac{Y_p - Y_s}{\sqrt{(X_p - X_s)^2 + (Y_p - Y_s)^2 + (Z_p - Z_s)^2}}\ ,$$

$$n = \frac{Z_p - Z_s}{\sqrt{(X_p - X_s)^2 + (Y_p - Y_s)^2 + (Z_p - Z_s)^2}}\ . \tag{2}$$

Now let $\underset{\sim}{A} = (a_{ij})$ be the rotation matrix by which a free vector in the X, Y, Z system is transformed into its x, y, z system equivalent, that is, for any vector $\vec{T}$, we have

$$\begin{bmatrix} x_T \\ y_T \\ z_T \end{bmatrix} = \begin{bmatrix} a_{11} & a_{12} & a_{13} \\ a_{21} & a_{22} & a_{23} \\ a_{31} & a_{32} & a_{33} \end{bmatrix} \cdot \begin{bmatrix} X_T \\ Y_T \\ Z_T \end{bmatrix}\ .$$

Using this relation, we obtain

$$\ell_I = a_{11}\ell + a_{12}m + a_{13}n$$
$$m_I = a_{21}\ell + a_{22}m + a_{23}n$$
$$n_I = a_{31}\ell + a_{32}m + a_{33}n \quad ,$$

so that

$$\frac{\ell_I}{n_I} = \frac{a_{11}\ell + a_{12}m + a_{13}n}{a_{31}\ell + a_{32}m + a_{33}n} \quad ,$$

$$\frac{m_I}{n_I} = \frac{a_{21}\ell + a_{22}m + a_{23}n}{a_{31}\ell + a_{32}m + a_{33}n} \quad . \tag{3}$$

Substituting the expressions in equations (2) for l, m, n into equations (3) and substituting the resultant expressions into equations (1), we obtain

$$x_I - d\cdot\frac{a_{11}(X_P - X_S) + a_{12}(Y_P - Y_S) + a_{13}(Z_P - Z_S)}{a_{31}(X_P - X_S) + a_{32}(Y_P - Y_S) + a_{33}(Z_P - Z_S)} = 0 ,$$

$$y_I - d\cdot\frac{a_{21}(X_P - X_S) + a_{22}(Y_P - Y_S) + a_{23}(Z_P - Z_S)}{a_{31}(X_P - X_S) + a_{32}(Y_P - Y_S) + a_{33}(Z_P - Z_S)} = 0 . \tag{4}$$

The equations (4) are our condition equations, two for each identifiable landmark. Now let us examine these equations and see what are the known and unknown quantities. Presumably we know d, the projection distance. We will also know x_I and y_I by direct measurement; X_p, Y_p, Z_p are calculable from the latitude and longitude of the landmark (and the time of the picture, if we are in an inertial system), obtainable from maps or an atlas. We do not know the satellite location X_s, Y_s, Z_s nor do we know the rotation matrix coefficients a_{11}, a_{12}, ..., a_{33}. These latter, however, are expressible in terms of a lesser number of rotation angles, such as the Eulerian angles Θ, ϕ, ψ illustrated in Figure 2.

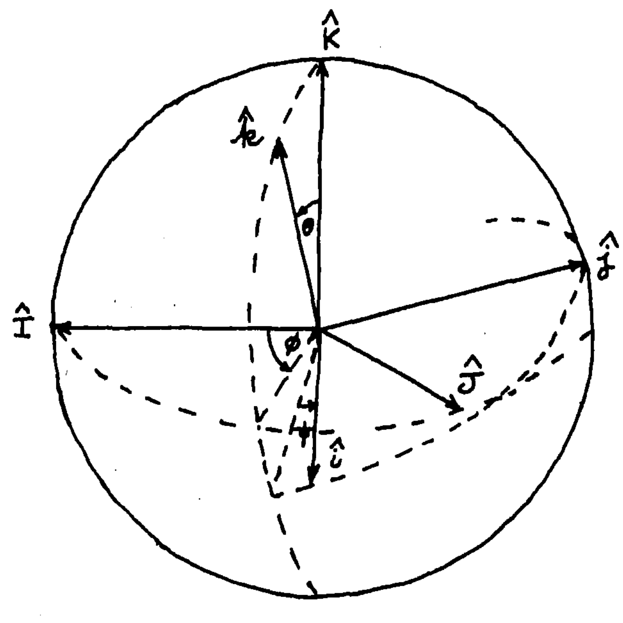

Figure 2.--The Eulerian angles.

In terms of Θ, ϕ, ψ, we would have

$$a_{11} = \cos\theta \cos\phi \cos\psi - \sin\phi \sin\psi \;,$$

$$a_{12} = \cos\theta \sin\phi \cos\psi + \cos\phi \sin\psi \;, \quad \text{etc.}$$

These rotation angles may be considered an expression of the satellite attitude.

Summing up, we have a total of six unknown quantities--X_s, Y_s, Z_s and Θ, ϕ, ψ--which are the same for each landmark, and we have two independent equations for each landmark. Therefore, a picture with four or more landmarks will overdetermine the six unknowns. This overdetermination permits us to employ least-squares iterative methods and to obtain successively better approximations to the six unknowns, starting from some initial guesses or estimates of their values. A detailed description of the procedure will be postponed to the discussion of the second approach; anyone interested in the special application of least-squares methods to this particular approach should consult Duane Brown's excellent monograph (1957) on the subject. Essentially one makes educated guesses as to the unknown parameters and utilizes the least-squares procedure to compute corrections to these estimates. The procedure is then iterated to the extent warranted by the desired degree of covergence.

TESTING AND RESULTS

The feasibility of the abovementioned approach was tested utilizing a "paper" (i.e., computer-simulated) satellite viewing 23 well-distributed hypothetical landmarks (fig. 3). The theory previously considered is, however, a "snapshot" theory --the image on the photographic plate represents the landmarks as seen simultaneously by the satellite at some given instant of time. The situation for a spin-scan camera is considerably different. The picture consists of a series of stepped scans (one per satellite-spin revolution); approximately 20 minutes separate the times of the first and the last scan.

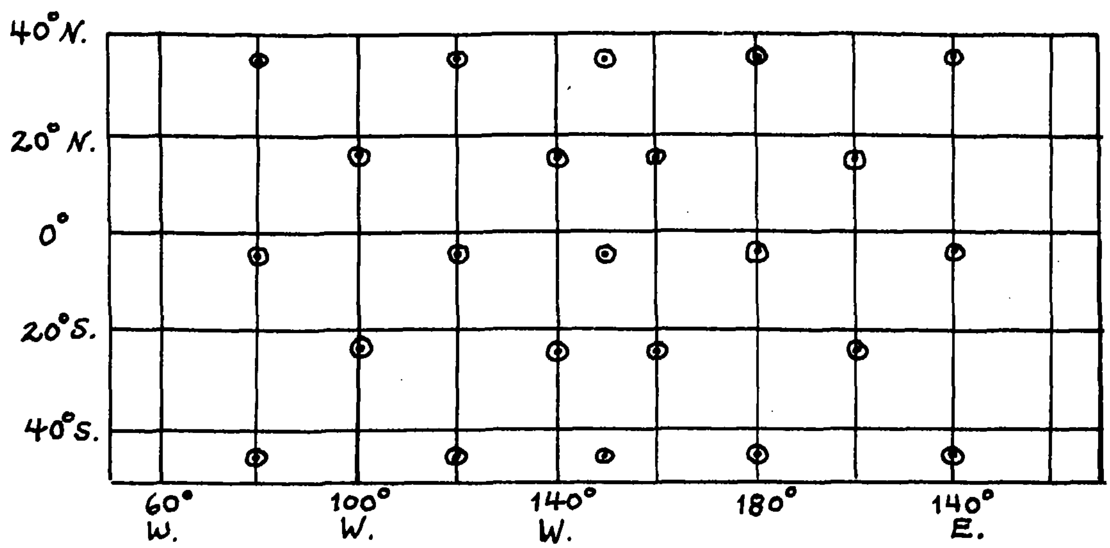

Figure 3.--Landmark configuration used in testing.

A truly geostationary satellite has, by definition, a fixed position in geographic space. Its spin axis, however, is fixed in inertial space, which results in a complete rotation (precession) of this axis in geographic space every siderial day. Because of this precession it became expedient to introduce a time-dependent rotational matrix into the position-attitude determination software to change the original sample and line numbers into the values they would assume were the spin axis nonrotating. This was easily accomplished and initial testing for a zero-inclination angle "paper" satellite exhibited excellent convergence properties. A more extensive series of tests was then devised, with small random discrepancies introduced into the line and sample numbers to simulate the inevitable imprecision characteristic of real data. These discrepancies tend to approximate the effects of moderate line and frame synchronization jitter, of errors in reading the landmark coordinates, etc., under fairly good operating conditions.

Because no real satellite is perfectly geostationary, and with the passage of time (and the diminishing amount of gas available for manuevering) becomes less geostationary, it was decided to run tests using a series of satellite inclination angles; the other orbital elements of the "paper" satellite were those then current for ATS-1. The first inclination angle was i=0° (the geostationary case), and the last was i=1°.609 (the current ATS-1 value). The results are tabulated in table 1.

Although the results reflect to some extent the randomness of the discrepancies introduced, several observations may be made. On the one hand, the computed subpoint location is relatively unaffected by the inclined orbits. On the other, the calculated earth-satellite distance and the spin-axis right ascension and declination solutions are very significantly influenced by these orbits, the discrepancies tending to increase with the inclination of the orbit. For this reason, and also bearing in mind that the landmark distribution of figure 3 is likely to be far better than anything actually encountered, it was decided that this approach could not be recommended as an operational procedure. Also, experience with ATS-1 suggested that operating conditions are usually considerably less favorable than those simulated above.

Table 1--Test results for 23 well-distributed points
(latitudes positive North; longitudes positive East)

Incl. = 0°	Initial guess	Computed	True	Discrepancy
Spin-axis R.A.	335°.0000	339°.5875	338°.9310	0°.6565
Spin-axis Decl.	88°.0000	86°.3626	86°.3280	0°.0346
Subpt. lat.	-1°.0000	0°.0470	0°.0000	0°.0470
Subpt. long.	-151°.0000	-149°.9028	-149°.9252	0°.0224
Radius vector	41,000.00(km)	42,184.09	42,159.20	24.89(km)

Incl. = 0°.10	Initial guess	Computed	True	Discrepancy
Spin-axis R.A.	335°.0000	340°.5932	338°.9310	1°.6622
Spin-axis Decl.	88°.0000	86°.3767	86°.3280	0°.0487
Subpt. lat.	-1°.0000	-0°.0124	0°.0221	-0°.0345
Subpt. long.	-151°.0000	-149°.8675	-149°.9240	0°.0565
Radius vector	41,000.00(km)	41,628.96	42,159.20	-530.24(km)

Incl. = 0°25	Initial guess	Computed	True	Discrepancy
Spin-axis R.A.	335°0000	337°6626	338°9310	-1°2684
Spin-axis Decl.	88°0000	86°2579	86°3280	-0°0701
Subpt. lat.	-1°0000	0°0023	0°0553	-0°0530
Subpt. long.	-151°0000	-149°9678	-149°9242	-0°0436
Radius vector	41,000.00(km)	41,877.59	42,159.19	-281.60(km)

Incl. = 0°50	Initial guess	Computed	True	Discrepancy
Spin-axis R.A.	335°0000	336°6034	338°9310	-2°3276
Spin-axis Decl.	88°0000	86°2373	86°3280	-0°0907
Subpt. lat.	-1°0000	0°0698	0°1106	-0°0408
Subpt. long.	-151°0000	-149°8947	-149°9247	0°0300
Radius vector	41,000.00(km)	41,628.73	42,159.19	-530.46(km)

Incl. = 1°00	Initial guess	Computed	True	Discrepancy
Spin-axis R.A.	335°0000	332°8383	338°9310	-6°0927
Spin-axis Decl.	88°0000	86°0706	86°3280	-0°2574
Subpt. lat.	-1°0000	0°2109	0°2211	-0°0102
Subpt. long.	-151°0000	-149°9189	-149°9265	0°0076
Radius vector	41,000.00(km)	41,158.77	42,159.17	-1,000.40(km)

Incl. = 1°609*	Initial guess	Computed	True	Discrepancy
Spin-axis R.A.	335°0000	326°4830	338°9310*	-12°4480
Spin-axis Decl.	88°0000	85°7066	86°3280*	-0°6214
Subpt. lat.	-1°0000	0°2942	0°3557*	-0°0615
Subpt. long.	-151°0000	-149°9626	-149°9301*	-0°0325
Radius vector	41,000.00(km)	41,214.83	42,159.15*	-944.32(km)

* Actual values for ATS-1 at one time.

A MORE GENERAL APPROACH

It is seen that the classical central projection theory is inadequate for determining simultaneously the attitude and position of current geostationary satellites because such satellites are really only approximately geostationary; their excursion in latitude during the 20-minute scanning period required for the picture is sufficient to destroy the coherency of the data. Because of this, some other approach whose validity would be independent of the motion of the satellite was sought. The most reasonable approach seemed to be to try to determine the elements of the orbit for a given epoch, together with the attitude vector. The position at any subsequent time could then be computed with the available orbital prediction software, while the attitude vector presumably would remain unchanged.

We would try to solve then for eight variables:

a, the semimajor axis;
ε, the eccentricity of the orbit;
i, the inclination angle;
ω, the argument of perigee;
Ω, the right ascension of the ascending node;
m, the mean anomaly at the epoch T_0;
α, the right ascension of the positive spin vector; and
Δ, the declination of the positive spin vector.

About this time it became known from the research of Doolittle et al. (1970) that for ATS-1 some nonlinear longitudinal shifting of the vectors represented by the central sample numbers was taking place. To avoid this source of error, it was suggested by Doolittle et al. that only the line numbers (rather than both line and sample numbers) of the observed landmarks be used in the determination. Also, because of the sensitivity of the orbital elements to the data from which they are computed, it was decided to use the data from a series of pictures covering a good-sized sector of an orbit. It was assumed that the cumulative effect of the perturbing forces during this period of time would be sufficiently small to permit the use of the classical two-body motion approximation.

LEAST-SQUARES ELEMENTS: THEORY

Each scan line corresponds to a certain angular displacement: Let ν be the number of radians per line. Then, if j is the line number for a landmark and j_{CL} the line number for the scan perpendicular to the spin axis, the cosine of the angle between the positive spin axis and a vector extending from the satellite to the landmark is given by

$$\cos\theta' = \sin\{\nu(j_{cL} - j)\} \quad . \tag{5}$$

If this angle is computed in terms of the unknown parameters, that is,

$$\theta = \theta(a, \varepsilon, i, \omega, \Omega, m, \alpha, \Delta) \quad ,$$

then our condition equation may be written

$$f = \cos\theta - \cos\theta' = 0 \tag{6}$$

where the primed angle represents the angle as computed from the observed line number and the unprimed angle represents the angle as computed from the unknown parameters.

If a_0, ε_0, i_0, ω_0, Ω_0, m_0, α_0, and Δ_0 are good estimates of a, ε, i, ω, Ω, m, α, and Δ, all at the epoch T_0, we may write to a sufficient approximation

$$f(a,\varepsilon,i,\omega,\Omega,m,\alpha,\Delta,j) = f(a_0,\varepsilon_0,i_0,\omega_0,\Omega_0,m_0,\alpha_0,\Delta_0,j) + \left.\frac{\partial f}{\partial a}\right|_0 \delta a + \left.\frac{\partial f}{\partial \varepsilon}\right|_0 \delta\varepsilon + \left.\frac{\partial f}{\partial i}\right|_0 \delta i + \left.\frac{\partial f}{\partial \omega}\right|_0 \delta\omega + \left.\frac{\partial f}{\partial \Omega}\right|_0 \delta\Omega + \left.\frac{\partial f}{\partial m}\right|_0 \delta m + \left.\frac{\partial f}{\partial \alpha}\right|_0 \delta\alpha + \left.\frac{\partial f}{\partial \Delta}\right|_0 \delta\Delta$$

where $a = a_0 + \delta a$, $\varepsilon = \varepsilon_0 + \delta\varepsilon$, etc.
Let $f_0 = f(a_0, ----, \Delta_0, j)$. Then, because $f(a, ---, \Delta, j) = 0$, we may write

$$f_0 + \left.\frac{\partial f}{\partial a}\right|_0 \delta a + -------- + \left.\frac{\partial f}{\partial \Delta}\right|_0 \delta\Delta = 0 .$$

There will be N such equations, one for each landmark. If we define

$$f_{0i} \equiv f(a_0,\varepsilon_0,i_0,\omega_0,\Omega_0,m_0,\alpha_0,\Delta_0,j_i) \quad , \tag{7}$$

these equations may be written

$$f_{oi} + \frac{\partial f}{\partial a}\bigg|_{oi}\delta a + \text{--------} + \frac{\partial f}{\partial \Delta}\bigg|_{oi}\delta \Delta = r_i \tag{8}$$

where r_i is the ith residual. From equations (5) and (6), we see that

$$\frac{\partial f}{\partial a} = \frac{\partial}{\partial a}(\cos\theta), \text{----------------}, \frac{\partial f}{\partial \Delta} = \frac{\partial}{\partial \Delta}(\cos\theta)$$

Now

$$\cos\theta_i = l_s l_i + m_s m_i + n_s n_i \tag{9}$$

where l_s, m_s, n_s are the satellite spin-vector direction cosines and l_i, m_i, n_i are the direction cosines of the satellite--ith landmark vector. We have

$$l_s = \cos\alpha\cos\Delta, \qquad m_s = \sin\alpha\cos\Delta, \qquad n_s = \sin\Delta, \tag{10}$$

and

$$l_i = \frac{x_i - X_i}{\sqrt{(x_i - X_i)^2 + (y_i - Y_i)^2 + (z_i - Z_i)^2}},$$

$$m_i = \frac{y_i - Y_i}{\sqrt{(x_i - X_i)^2 + (y_i - Y_i)^2 + (z_i - Z_i)^2}},$$

$$n_i = \frac{z_i - Z_i}{\sqrt{(x_i - X_i)^2 + (y_i - Y_i)^2 + (z_i - Z_i)^2}} \tag{11}$$

where (x_i, y_i, z_i) is the landmark position and (X_i, Y_i, Z_i) is the satellite position, both in inertial space at the time the ith landmark is scanned.

Let us show how f_{oi} and $\frac{\partial f}{\partial a}\Big|_{oi}$ are actually computed--the expressions and computational procedure for $\frac{\partial f}{\partial \varepsilon}\Big|_{oi}$, $\frac{\partial f}{\partial i}\Big|_{oi}$, etc. should then be easily derivable by the interested reader.

Suppose we have a landmark (the ith one) on an ATS-type picture. We find the line number j_i passing through the landmark. Finding the picture start-time and the satellite spin-rate, we compute the time (elapsed since our chosen epoch T_0) corresponding to j_i,

$$\Delta t = (j_i \div \text{spin rate}) + \text{picture start time} - T_0. \tag{12}$$

Obtaining an ephemeris, we express T_0 as its sidereal equivalent; the time since the epoch is also expressed in sidereal units,

$$\Delta t = 1.0027379093 \times \Delta t_{(\text{mean solar})} \; .$$

Using a good map, we determine the latitude and longitude (ϕ_{gd}, λ) of the landmark, changing the latitude (which is geodetic) into its geocentric equivalent by means of the equation

$$\begin{aligned}\phi = \phi_{gd} - 0.00335851579910756 \sin(2\phi_{gd}) &+ 0.000005639814186428 \sin(4\phi_{gd}) \\ &- 0.000000012627603366 \sin(6\phi_{gd}) \\ &+ 0.0000000000031807504 \sin(8\phi_{gd}) \; .\end{aligned} \tag{13}$$

Defining the constant $K_T = 2\pi /$ sidereal day, we compute x_i, y_i, z_i,

$$x_i = \frac{a_\oplus b_\oplus \cos\phi_i \cos(\lambda_i + K_T(T_0 + \Delta t))}{\sqrt{a_\oplus^2 \sin^2\phi_i + b_\oplus^2 \cos^2\phi_i}},$$

$$y_i = \frac{a_\oplus b_\oplus \cos\phi_i \sin(\lambda_i + K_T(T_0 + \Delta t))}{\sqrt{a_\oplus^2 \sin^2\phi_i + b_\oplus^2 \cos^2\phi_i}},$$

$$z_i = \frac{a_\oplus b_\oplus \sin\phi_i}{\sqrt{a_\oplus^2 \sin^2\phi_i + b_\oplus^2 \cos^2\phi_i}}, \tag{14}$$

where $a_\oplus$ and $b_\oplus$ are the semimajor and semiminor axes of the earth, respectively, the λ_i is considered positive eastward. We note that K_T ($T_0 + \Delta t$) is the Greenwich Hour Angle (G.H.A.) at the time the landmark is scanned.

To determine the position of the satellite in inertial space, we must first ascertain its eccentric anomaly E_i when the ith landmark is scanned. We define the satellite's <u>mean</u> motion as

$$n_0 \equiv 0.07436574 \times (6378.270)^{3/2} \times a_0^{-3/2} \tag{15}$$

and solve Kepler's Equation

$$E_i - \varepsilon_o \sin E_i = m_o + n_o \Delta t \text{ (mean solar)} \tag{16}$$

for E_i; various iterative schemes for accomplishing this are extant in the literature. The a_o, ε_o and m_o are initial orbital element estimates. Using this computed value of E_i, we may compute

Also, from here on, the semimajor axis should be considered as being expressed in earth radius units of 6378.270 km.

$$\begin{aligned}
X_i &= a_o(\cos\omega_o \cos\Omega_o - \sin\omega_o \sin\Omega_o \cos i_o)(\cos E_i - \varepsilon_o) \\
&\quad - a_o\sqrt{1-\varepsilon_o^2}(\sin\omega_o \cos\Omega_o + \cos\omega_o \sin\Omega_o \cos i_o)\sin E_i \ , \\
Y_i &= a_o(\cos\omega_o \sin\Omega_o + \sin\omega_o \cos\Omega_o \cos i_o)(\cos E_i - \varepsilon_o) \\
&\quad + a_o\sqrt{1-\varepsilon_o^2}(-\sin\omega_o \sin\Omega_o + \cos\omega_o \cos\Omega_o \cos i_o)\sin E_i \ , \\
Z_i &= a_o(\sin\omega_o \sin i_o)(\cos E_i - \varepsilon_o) + a_o\sqrt{1-\varepsilon_o^2}\cos\omega_o \sin i_o \sin E_i \ .
\end{aligned} \tag{17}$$

So finally, combining equations (5), (6), (7), (10), and (11), we obtain for f_{oi},

$$f_{oi} = \frac{(x_i - X_i)\cos\alpha_o \cos\Delta_o + (y_i - Y_i)\sin\alpha_o \cos\Delta_o + (z_i - Z_i)\sin\Delta_i}{\sqrt{(x_i - X_i)^2 + (y_i - Y_i)^2 + (z_i - Z_i)^2}} - \sin\{\nu(j_{ci} - j_i)\} \tag{18}$$

where x_i, y_i, z_i have the values computed from equations (14), and X_i, Y_i, Z_i are computed from equations (17).

Concerning the computation of $\left.\frac{\partial f}{\partial a}\right|_{oi}$, we have seen that $\frac{\partial f}{\partial a} = \frac{\partial(\cos\theta)}{\partial a}$ so by using equation (9), we obtain now

$$\begin{aligned}
\frac{\partial l_i}{\partial a_o} &= \frac{\partial l_i}{\partial X_i}\frac{\partial X_i}{\partial a_o} + \frac{\partial l_i}{\partial Y_i}\frac{\partial Y_i}{\partial a_o} + \frac{\partial l_i}{\partial Z_i}\frac{\partial Z_i}{\partial a_o} \ , \\
\frac{\partial m_i}{\partial a_o} &= \frac{\partial m_i}{\partial X_i}\frac{\partial X_i}{\partial a_o} + \frac{\partial m_i}{\partial Y_i}\frac{\partial Y_i}{\partial a_o} + \frac{\partial m_i}{\partial Z_i}\frac{\partial Z_i}{\partial a_o} \ , \\
\frac{\partial n_i}{\partial a_o} &= \frac{\partial n_i}{\partial X_i}\frac{\partial X_i}{\partial a_o} + \frac{\partial n_i}{\partial Y_i}\frac{\partial Y_i}{\partial a_o} + \frac{\partial n_i}{\partial Z_i}\frac{\partial Z_i}{\partial a_o} \ .
\end{aligned} \tag{19}$$

Defining $$R_i \equiv \sqrt{(x_i - X_i)^2 + (y_i - Y_i)^2 + (z_i - Z_i)^2} \tag{20}$$

and referring to equations (11), we obtain

$$\begin{aligned}
\frac{\partial l_i}{\partial X_i} &= -[(y_i - Y_i)^2 + (z_i - Z_i)^2]/R_i^3 , \\
\frac{\partial l_i}{\partial Y_i} &= (x_i - X_i)(y_i - Y_i)/R_i^3 , \\
\frac{\partial l_i}{\partial Z_i} &= (x_i - X_i)(z_i - Z_i)/R_i^3 , \\
\frac{\partial m_i}{\partial X_i} &= \frac{\partial l_i}{\partial Y_i} , \\
\frac{\partial m_i}{\partial Y_i} &= -[(x_i - X_i)^2 + (z_i - Z_i)^2]/R_i^3 , \\
\frac{\partial m_i}{\partial Z_i} &= (y_i - Y_i)(z_i - Z_i)/R_i^3 , \\
\frac{\partial n_i}{\partial X_i} &= \frac{\partial l_i}{\partial Z_i} , \\
\frac{\partial n_i}{\partial Y_i} &= \frac{\partial m_i}{\partial Z_i} , \\
\frac{\partial n_i}{\partial Z_i} &= -[(x_i - X_i)^2 + (y_i - Y_i)^2]/R_i^3 .
\end{aligned} \tag{21}$$

Using equations (17) and the relation

$$\frac{\partial E_i}{\partial a_o} = -\frac{3}{2}\,\frac{E_i - \varepsilon_o \sin E_i - m_o}{a_o(1 - \varepsilon_o \cos E_i)} \tag{22}$$

obtainable from Kepler's Equation (16), we obtain

$$\begin{aligned}
\frac{\partial X_i}{\partial a_o} = {} & \left[(\cos\omega_o \cos\Omega_o - \sin\omega_o \sin\Omega_o \cos i_o)\cdot\left(\cos E_i - \varepsilon_o + \frac{3}{2}\sin E_i \cdot \frac{E_i - \varepsilon_o \sin E_i - m_o}{1 - \varepsilon_o \cos E_i}\right)\right] \\
& - \left[\sqrt{1-\varepsilon_o^2}\,(\sin\omega_o \cos\Omega_o + \cos\omega_o \sin\Omega_o \cos i_o)\cdot\left(\sin E_i - \frac{3}{2}\cos E_i \cdot \frac{E_i - \varepsilon_o \sin E_i - m_o}{1 - \varepsilon_o \cos E_i}\right)\right] , \\
\frac{\partial Y_i}{\partial a_o} = {} & \left[(\cos\omega_o \sin\Omega_o + \sin\omega_o \cos\Omega_o \cos i_o)\cdot\left(\cos E_i - \varepsilon_o + \frac{3}{2}\sin E_i \cdot \frac{E_i - \varepsilon_o \sin E_i - m_o}{1 - \varepsilon_o \cos E_i}\right)\right] \\
& + \left[\sqrt{1-\varepsilon_o^2}\,(-\sin\omega_o \sin\Omega_o + \cos\omega_o \cos\Omega_o \cos i_o)\cdot\left(\sin E_i - \frac{3}{2}\cos E_i \cdot \frac{E_i - \varepsilon_o \sin E_i - m_o}{1 - \varepsilon_o \cos E_i}\right)\right] , \\
\frac{\partial Z_i}{\partial a_o} = {} & \left[(\sin\omega_o \sin i_o)\cdot\left(\cos E_i - \varepsilon_o + \frac{3}{2}\sin E_i \cdot \frac{E_i - \varepsilon_o \sin E_i - m_o}{1 - \varepsilon_o \cos E_i}\right)\right] \\
& + \left[\sqrt{1-\varepsilon_o^2}\,(\cos\omega_o \sin i_o)\cdot\left(\sin E_i - \frac{3}{2}\cos E_i \cdot \frac{E_i - \varepsilon_o \sin E_i - m_o}{1 - \varepsilon_o \cos E_i}\right)\right] .
\end{aligned} \tag{23}$$

To evaluate $\left.\frac{\partial f}{\partial a}\right|_{oi}$, one then computes $\frac{\partial l_i}{\partial X_i}, \frac{\partial l_i}{\partial Y_i}$, - - - - - - - -, $\frac{\partial n_i}{\partial Z_i}$ using equations (20) and (21), and $\frac{\partial X_i}{\partial a_o}, \frac{\partial Y_i}{\partial a_o}, \frac{\partial Z_i}{\partial a_o}$ using equations (23); one will also use the previously calculated values of x_i, y_i, z_i, X_i, Y_i, Z_i, and E_i in this computation. Using these values and equations (19) enables us to compute $\frac{\partial l_i}{\partial a_o}$, $\frac{\partial m_i}{\partial a_o}$, and $\frac{\partial n_i}{\partial a_o}$. Using equations (10), we may then finally calculate

$$\left.\frac{\partial f}{\partial a}\right|_{oi} = (\cos\alpha_o \cos\Delta_o)\frac{\partial l_i}{\partial a_o} + (\sin\alpha_o \cos\Delta_o)\frac{\partial m_i}{\partial a_o} + \sin\Delta_o \frac{\partial n_i}{\partial a_o} \tag{24}$$

In a similar manner, one may derive expressions for and calculate

$$\left.\frac{\partial f}{\partial \varepsilon}\right|_{oi}, \left.\frac{\partial f}{\partial i}\right|_{oi}, \left.\frac{\partial f}{\partial \omega}\right|_{oi}, \left.\frac{\partial f}{\partial \Omega}\right|_{oi}, \left.\frac{\partial f}{\partial m}\right|_{oi}, \left.\frac{\partial f}{\partial \alpha}\right|_{oi}, \text{ and } \left.\frac{\partial f}{\partial \Delta}\right|_{oi} .$$

Having computed all these quantities, let us look again at equation (8),

$$f_{oi} + \left.\frac{\partial f}{\partial a}\right|_{oi} \delta a + \text{------} + \left.\frac{\partial f}{\partial \Delta}\right|_{oi} \delta\Delta = r_i .$$

The theory of least squares postulates that

$$\begin{aligned}
&\frac{\partial}{\partial(\delta a)}\left(\sum_i^N w_i r_i^2\right) = 0 , \\
&\frac{\partial}{\partial(\delta \varepsilon)}\left(\sum_i^N w_i r_i^2\right) = 0 , \\
&\text{------------} , \\
&\frac{\partial}{\partial(\delta \Delta)}\left(\sum_i^N w_i r_i^2\right) = 0 ,
\end{aligned} \tag{25}$$

where w_i is the <u>weight</u> of the ith condition equation and N is the total number of landmarks. From this, we obtain

$$\sum_i^N w_i r_i \frac{\partial r_i}{\partial(\delta a)} = \sum_i^N w_i r_i \frac{\partial r_i}{\partial(\delta \varepsilon)} = \text{-----------} = \sum_i^N w_i r_i \frac{\partial r_i}{\partial(\delta \Delta)} = 0 .$$

But from equation (8), we have $\frac{\partial r_i}{\partial(\delta a)} = \frac{\partial f}{\partial a}\Big|_{oi}$, $\frac{\partial r_i}{\partial(\delta \varepsilon)} = \frac{\partial f}{\partial \varepsilon}\Big|_{oi}$, etc.

So equations (25) finally reduce to

$$\sum_i^N w_i r_i \frac{\partial f}{\partial a}\Big|_{oi} = 0,$$
$$\sum_i^N w_i r_i \frac{\partial f}{\partial \varepsilon}\Big|_{oi} = 0,$$
$$\sum_i^N w_i r_i \frac{\partial f}{\partial i}\Big|_{oi} = 0, \text{ etc.} \tag{26}$$

Substituting for r_i on the right side of equation (8), we obtain

$$\Big(\sum_i^N w_i \frac{\partial f}{\partial a}\Big|_{oi}^2\Big)\delta a + \Big(\sum_i^N w_i \frac{\partial f}{\partial a}\Big|_{oi}\frac{\partial f}{\partial \varepsilon}\Big|_{oi}\Big)\delta\varepsilon + \text{-----------} + \Big(\sum_i^N w_i \frac{\partial f}{\partial a}\Big|_{oi}\frac{\partial f}{\partial \Delta}\Big|_{oi}\Big)\delta\Delta = -\sum_i^N w_i \frac{\partial f}{\partial a}\Big|_{oi} f_{oi},$$
$$\Big(\sum_i^N w_i \frac{\partial f}{\partial \varepsilon}\Big|_{oi}\frac{\partial f}{\partial a}\Big|_{oi}\Big)\delta a + \Big(\sum_i^N w_i \frac{\partial f}{\partial \varepsilon}\Big|_{oi}^2\Big)\delta\varepsilon + \text{-----------} + \Big(\sum_i^N w_i \frac{\partial f}{\partial \varepsilon}\Big|_{oi}\frac{\partial f}{\partial \Delta}\Big|_{oi}\Big)\delta\Delta = -\sum_i^N w_i \frac{\partial f}{\partial \varepsilon}\Big|_{oi} f_{oi},$$
$$\text{--},$$
$$\text{--},$$
$$\Big(\sum_i^N w_i \frac{\partial f}{\partial \Delta}\Big|_{oi}\frac{\partial f}{\partial a}\Big|_{oi}\Big)\delta a + \Big(\sum_i^N w_i \frac{\partial f}{\partial \Delta}\Big|_{oi}\frac{\partial f}{\partial \varepsilon}\Big|_{oi}\Big)\delta\varepsilon + \text{-----------} + \Big(\sum_i^N w_i \frac{\partial f}{\partial \Delta}\Big|_{oi}^2\Big)\delta\Delta = -\sum_i^N w_i \frac{\partial f}{\partial \Delta}\Big|_{oi} f_{oi}. \tag{27}$$

We have then eight linear equations with eight unknowns, that is

$$a_{11}\delta a + a_{12}\delta\varepsilon + a_{13}\delta i + a_{14}\delta\omega + a_{15}\delta\Omega + a_{16}\delta m + a_{17}\delta\alpha + a_{18}\delta\Delta = c_1,$$
$$a_{21}\delta a + a_{22}\delta\varepsilon + a_{23}\delta i + a_{24}\delta\omega + a_{25}\delta\Omega + a_{26}\delta m + a_{27}\delta\alpha + a_{28}\delta\Delta = c_2,$$
$$\text{--},$$
$$\text{--},$$
$$a_{81}\delta a + a_{82}\delta\varepsilon + a_{83}\delta i + a_{84}\delta\omega + a_{85}\delta\Omega + a_{86}\delta m + a_{87}\delta\alpha + a_{88}\delta\Delta = c_8 \tag{28}$$

where from equations (27)

$$a_{11} \equiv \sum_i^N w_i \frac{\partial f}{\partial a}\Big|_{oi}^2,\quad a_{12} \equiv \sum_i^N w_i \frac{\partial f}{\partial a}\Big|_{oi}\frac{\partial f}{\partial \varepsilon}\Big|_{oi},\ \text{-------------},\ a_{88} \equiv \sum_i^N w_i \frac{\partial f}{\partial \Delta}\Big|_{oi}^2,$$
$$c_1 \equiv -\sum_i^N w_i \frac{\partial f}{\partial a}\Big|_{oi} f_{oi},\quad c_2 \equiv -\sum_i^N w_i \frac{\partial f}{\partial \varepsilon}\Big|_{oi} f_{oi},\ \text{-------------},\ c_8 \equiv -\sum_i^N w_i \frac{\partial f}{\partial \Delta}\Big|_{oi} f_{oi}. \tag{29}$$

Having already computed f_{oi}, $\left.\frac{\partial f}{\partial a}\right|_{oi}$, ---, $\left.\frac{\partial f}{\partial \Delta}\right|_{oi}$ for every value of i, we may use their values and calculate all the a_{ij}'s and c_i's; δa, $\delta \varepsilon$, δi, $\delta \omega$, $\delta \Omega$, δm, $\delta \alpha$, and $\delta \Delta$ may then be computed at once through the use of determinants, and the values obtained used to compute improved estimates of $a, \varepsilon, \ldots, \alpha, \Delta$ by means of $a = a_o + \delta a$, $\varepsilon = \varepsilon_o + \Delta\varepsilon$, etc. The entire process may then be iterated until a satisfactory degree of convergence is obtained.

TESTING AND RESULTS

Using the preceding considerations, a computer program for determining orbital elements was originated and debugged for use on a CDC 6600 computer. Initial testing with multiple-pass data from a "paper" satellite yielded satisfactory results at first, i.e., perfect data generated by a hypothetical satellite with known attitude and orbital characteristics together with estimates of a, ε, i, ω, Ω, m, α, and Δ, when used as input for the program in question, resulted in perfect convergence to these same a priori values of a, ε, i, ω, Ω, m, α, and Δ. As with the previous approach, it was decided to simulate reality more faithfully by introducing small random discrepancies into the data. This situation resulted in considerable aberration in the elements computed from these data. In particular, because the orbit under test was nearly circular, the argument of perigee and the mean anomaly at the epoch were mutually poorly defined, and the discrepancies for these elements, arising from the randomness, were correspondingly gross.

It was determined that because the orbit was very nearly circular, very little error in mapping a picture would result if the argument of perigee was arbitrarily defined as some fixed quantity (this would effectively determine the mean anomaly at the epoch very closely) and the eccentricity was set = 0. With these provisions, the errors in the other elements were considerably diminished, but not so much as to allay fears about their magnitude in an actual nonhypothetical situation. The situation indicated the need for an experimental test with a real satellite to see if the elements other than the argument of perigee and the eccentricity, and the spin vector, could be satisfactorily determined.

Accordingly, on June 14, 1970, a series of seven ATS-3 spin-scan pictures were taken between 1349 and 1957 Universal Time (U.T.). A typical picture is shown in figure 4. Seventy-nine landmarks were selected from this series of pictures. Software existed for enhancing a small sector of such a picture; figure 5 shows an enhanced landmark sector of the Baja California area. Such sectors enable one to determine easily the line and sample numbers corresponding to a given landmark, and so were used throughout for this purpose.

Figure 4.--ATS-3 spin-scan picture.

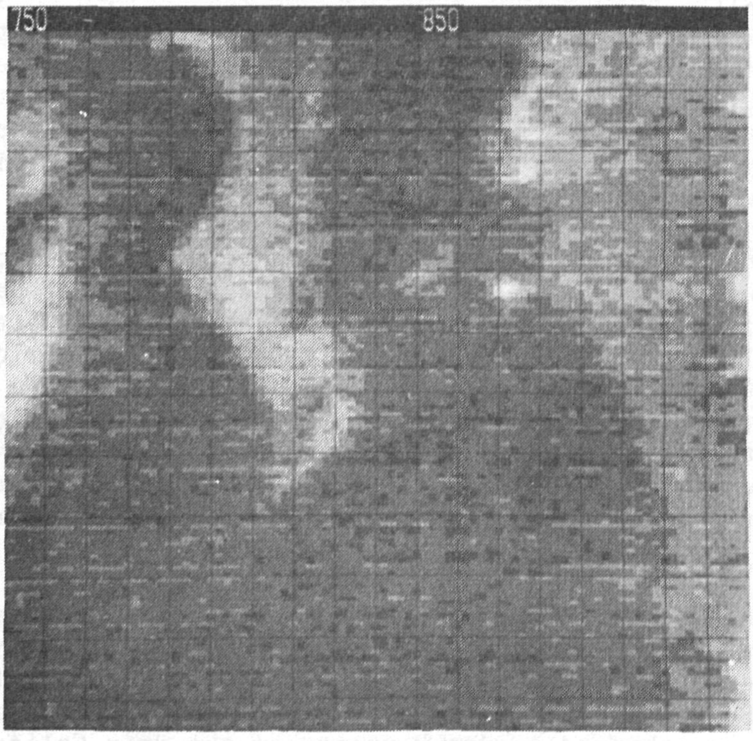

Figure 5.--Enhanced landmark sector of Baja California.

At about the time of these tests, certain information on anomalies of the ATS-3 spin axis was published by H. Ausfresser (1970). Briefly, it had been determined that the actual spin axis of ATS-3 no longer coincided with the satellite's geometrical axis. As a result, it became necessary to interpose an additional matrix multiplication in the previous chain of logic, the pertinent rotational matrix being that required to ensure coherent data.

Because we envision in actual operations that the landmark selection would be made by subprofessional personnel, hand-massaging of the data was scrupulously avoided; all landmarks chosen were assigned the same weight, with no arbitrary subsequent rejections directed toward a "good" answer. Using as initial estimates the known orbital elements and spin-axis right ascension and declination, various attempts to secure convergence to the proper values of a, i, $\omega, \Omega, \alpha, \Delta$ were undertaken. Unfortunately, every such attempt resulted in divergence.

THOUGHTS

An account of the reasons for the failure of the second approach for position and attitude determination and the corresponding suggestions for improved future results follow.

a. The spin-scan picture start-times were known only to the nearest minute. An uncertainty of 1 minute of time translates into an uncertainty of 15 minutes of arc, so improvement in start-time information is indicated.

b. With ATS-3, the line number of a given line can be determined only indirectly and with a certain degree of uncertainty corresponding to the location of the vertical-frame synchronization point. In the forthcoming SMS-GOES satellites, however, every line is to be directly attributable.

c. When specialized maps for a given area were not readily available, a standard atlas was used. Although positions were obtained as carefully as possible, some inaccuracy was inevitable. A more extensive set of cartographic references is indicated.

d. As previously indicated, the landmarks utilized were not identical in quality. An investigation of some reliable weighting scheme should ameliorate this situation.

e. The skewing of the ATS-3 spin axis was to some degree indeterminate; in any event, it is felt strongly that the influence of this canting on the final results was distinctly negative.

f. The orbit computed was a simple two-body motion ellipse. A more complex implementation of this computation, taking into account the action of perturbing forces during the series of passes, should yield improved results.

g. The orbital elements computed were the so-called classical orbital elements which are not always well defined. Solving for a less ambiguous set of elements might well make a significant difference in the final outcome.

None of these comments are intended to condemn completely the concept of using landmarks as input. It is felt that the use of landmarks for satellite attitude determination will continue to be a valuable tool for some time to come. Position determination, however, is another matter entirely. Even granting the aforementioned improvements, it is felt that the results obtained will be far inferior to those attainable with existing trilateration equipment. Also, the process of obtaining landmark sectors and from them line and sample numbers, together with the required geographic coordinates, etc., would require the on-the-spot presence of a large number of personnel with immediate and exclusive access to a digital computer and display device. If positions (elements) and attitudes of any current usefulness are to be obtained, the procedure would be both costly and tedious.

Some effort is currently being devoted to the automating of the landmark detection and input operations, using the concepts of pattern recognition theory. Until this automation takes place, the procedure will remain tedious and time-consuming. For this reason, it is felt that anyone contemplating further effort in this direction should consider the perfected software as a diagnostic tool rather than an operational procedure.

REFERENCES

"Applications Technology Satellite, Technical Data Report," NASA ATS Program, Goddard Spaceflight Center, March 1968.

Ausfresser, H., "Investigation of an ATS Attitude Anomaly," Contract NAS 5-21129, Westinghouse Corporation, July 1970.

Brown, Duane C., "A Treatment of Analytical Photogrammetry, with Emphasis on Ballistic Camera Applications," RCA Data Reduction Technical Report No. 39, ASTIA Document No. 124144, August 1957.

Doolittle, R. C., Bristor, C. L., and Lauritson, L., "Mapping of Geostationary Satellite Pictures--An Operational Experiment," NOAA Technical Memorandum NESCTM 20, March 1970.

(Continued from inside front cover)

NESCTM 20 Mapping of Geostationary Satellite Pictures - An Operational Experiment. R. C. Doolittle, C. L. Bristor and L. Lauritson, March 1970. (PB-191 189)

NESCTM 22 Publications and Final Reports on Contracts and Grants, 1969--NESC. Staff Members, January 1970. (PB-190 632)

NESCTM 23 Estimating Mean Relative Humidity From the Surface to 500 Millibars by Use of Satellite Pictures. Frank J. Smigielski and Lee M. Mace, March 1970. (PB-191 741)

NESCTM 24 Operational Brightness Normalization of ATS-1 Cloud Pictures. V. Ray Taylor, August 1970. (PB-194 638)

NESCTM 25 Aircraft Microwave Measurements of the Arctic Ice Pack. Alan E. Strong and Michael H. Fleming, August 1970. (PB-194 588)

NOAA Technical Memoranda

NESS 21 Geostationary Satellite Position and Attitude Determination Using Picture Landmarks. William J. Dambeck, August 1972.

NESS 26 Potential of Satellite Microwave Sensing for Hydrology and Oceanography Measurements. John C. Alishouse, Donald R. Baker, E. Paul McClain, and Harold W. Yates, March 1971. (COM-71-00544)

NESS 27 A Review of Passive Microwave Remote Sensing. James J. Whalen, March 1971.

NESS 28 Calculation of Clear-Column Radiances Using Airborne Infrared Temperature Profile Radiometer Measurements Over Partly Cloudy Areas. William L. Smith, March 1971. (COM-71-00556)

NESS 29 The Operational Processing of Solar Proton Monitor and Flat Plate Radiometer Data. Henry L. Phillips and Louis Rubin, (in preparation).

NESS 30 Limits on the Accuracy of Infrared Radiation Measurements of Sea-Surface Temperature From a Satellite. Charles Braun, December 1971.

NESS 31 Publications and Final Reports on Contracts and Grants, 1970--NESS. December 1971. (COM-72-10303)

NESS 32 On Reference Levels for Determining Height Profiles From Satellite-Measured Temperature Profiles. Christopher M. Hayden, December 1971. (COM-72-50393)

NESS 33 Use of Satellite Data in East Coast Snowstorm Forecasting. Frances C. Parmenter, February 1972. (COM-72-10482)

NESS 34 Chromium Dioxide Recording--Its Characteristics and Potential for Telemetry. Florence Nesh, March 1972.

NESS 35 Modified Version of the Improved TIROS Operational Satellite (ITOS D-G). A. Schwalb, April 1972.

NESS 36 A Technique for the Analysis and Forecasting of Tropical Cyclone Intensities From Satellite Pictures. Vernon F. Dvorak, May 1972.

NESS 37 Some Preliminary Results of 1971 Aircraft Microwave Measurements of Ice in the Beaufort Sea. Richard J. DeRycke and Alan E. Strong, June 1972.

NESS 38 Publications and Final Reports on Contracts and Grants, 1971--NESS. June 1972.

NESS 39 Operational Procedures For Estimating Wind Vectors From Geostationary Satellite Data. Michael T. Young, Russell C. Doolittle, and Lee M. Mace, July 1972.